

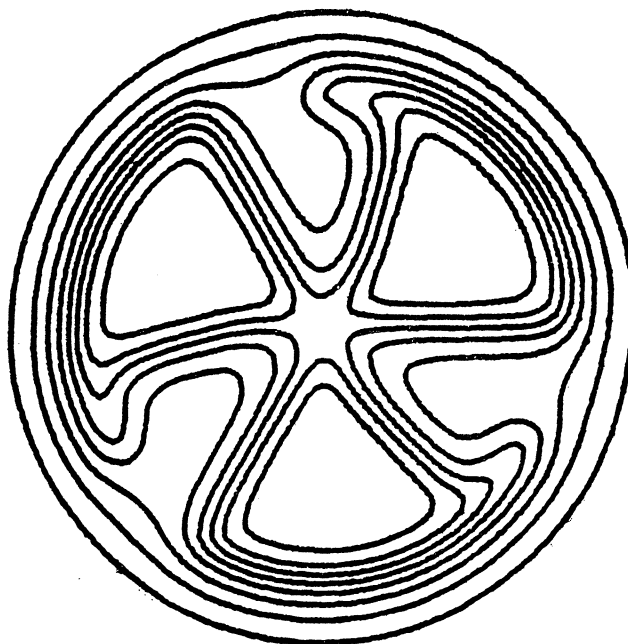
MICHIGAN STATE UNIVERSITY

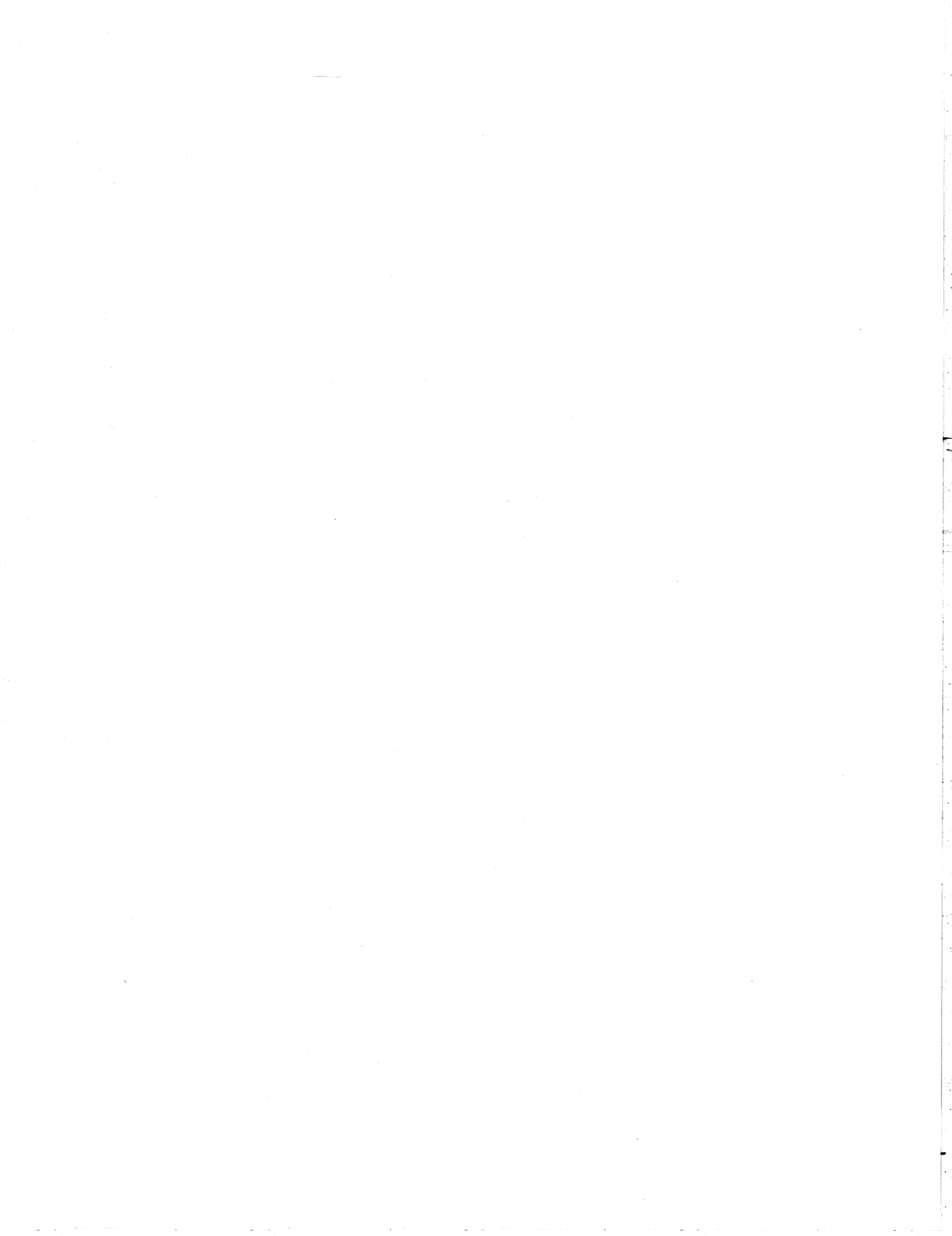
CYCLOTRON LABORATORY

OBSERVATION OF GIANT GAMOW-TELLER STRENGTH
IN (p, n) REACTIONS

R. R. DOERING, AARON GALONSKY, D. M. PATTERSON,

and G. F. BERTSCH





Observation of Giant Gamow-Teller Strength
in (p,n) Reactions*

R.R. Doering, Aaron Galonsky, D.M. Patterson,[†]
and

G.F. Bertsch

Cyclotron Laboratory, Department of Physics
Michigan State University, East Lansing, Michigan 48824

ABSTRACT

In $^{90}\text{Zr}(p,n)^{90}\text{Nb}$ spectra for $E_p=35$ and 45 MeV, we observe a strong enhancement of the $T=4$ continuum over a range of excitation energies (FWHM = 4.2 ± 0.4 MeV) centered at 8.4 ± 0.3 MeV. The data are consistent with an interpretation of the broad peak as a $(\pi g_{7/2}^{-1}, \nu g_{9/2}^{-1})_1^+$ excitation which corresponds to both the giant Gamow-Teller resonance and the anti-analog of the giant magnetic-dipole resonance. Similar structure is observed near the IAS of ^{48}Ca , ^{120}Sn , and ^{208}Pb .

Allowed β decays between nuclei with $N > Z$ are generally found to be hindered with respect to calculated single-particle rates.¹ An analogous phenomenon for electromagnetic transitions is understood in terms of the concentration of E1 strength near $E_x = 75/A^{1/3}$ MeV in the giant electric-dipole resonance.

The corresponding resonance which exhausts the Fermi β -decay strength to or from a $T_z = T$ ground state is its $T_z = T-1$ isobaric analog (IAS), first identified in nuclei heavier than the mirror pairs by Anderson and Wong² in 1961 via the (p,n) reaction. In 1963, Ikeda, Fujii, and Fujita³ suggested that the Gamow-Teller strength function may be similarly localized near the IAS as part of a badly-broken, but persistent, Wigner supermultiplet. However except possibly in light proton-rich nuclei,⁴ such a resonance has been heretofore unseen.¹ In this letter, we present evidence for the first direct observation of the giant Gamow-Teller resonance in nuclei with $N > Z$.

We have recently completed a series of (p,n)-IAS differential cross section measurements on targets of ^{48}Ca , ^{90}Zr , ^{120}Sn , and ^{208}Pb with 25-, 35-, and 45-MeV protons from the MSU cyclotron. These data have been acquired with conventional neutron time-of-flight and pulse-shape-discrimination techniques. Experimental details and the results of a microscopic distorted-wave-Born-approximation (DWBA) analysis of the (p,n)-IAS cross sections are available in a previous publication.⁵ Many of the neutron time-of-flight spectra reveal structure in addition to the IAS in the giant-resonance region. Such a spectrum, of neutrons

* Work supported by the National Science Foundation and the Office of Naval Research.

[†] Present address: Fusion Research Center, University of Texas, Austin, Texas 78712.

produced at a scattering angle of 0° from the bombardment of a ^{90}Zr target with 35-MeV protons, is shown in Fig. 1. The prominent peak around channel 400 is the isobaric analog of the target ground state. The neutron energy resolution in the vicinity of the IAS is approximately 170 keV, which should certainly be adequate to resolve several analogs of excited states (EAS) of ^{90}Zr . The expected positions of the first few are indicated in the figure. The apparent absence of EAS with even 5% as much as the IAS cross section (2.7 mb/sr) at this angle is an indication of the direct nature of the (p,n) reaction at $E_p=35$ MeV. Although the T=5 EAS are not prominent, there is an obvious enhancement of the T=4 background states over a broad region centered about 3 MeV in excitation energy above the IAS. Note that the low-excitation tail of this peak extends below the expected location of the first EAS.

We observe similar broad peaks near the IAS of ^{48}Ca , ^{120}Sn , and ^{208}Pb . For each target, the structure is most pronounced at the highest bombarding energy ($E_p=45$ MeV) and most-forward scattering angle ($\theta=0^\circ$). The dynamic ranges of our spectra at $E_p=25$ MeV do not always fully encompass these peaks; however, it appears that their cross sections are consistently much smaller for protons of such low energy.

The initial study has been directed toward analyzing the data from ^{90}Zr at $E_p=45$ MeV. Figure 2 displays differential cross section vs. neutron energy derived from the corresponding time-of-flight spectrum at $\theta=0^\circ$. As in the data for $E_p=35$ MeV, there is a peak at $E_x=8.4\pm 0.3$ MeV with a full width at half maximum of

4.2 ± 0.4 MeV. The errors in the centroid and width principally reflect uncertainties related to the choice of background. The cross section at each scattering angle ($\theta_{lab}=0^\circ, 10^\circ-85^\circ$ in 5 $^\circ$ steps) has been extracted by summing the $d^2\sigma/d\Omega dE$ spectrum above a linear background fit to regions adjacent to the broad peak (as shown in Fig. 2) and then subtracting the previously determined IAS $\sigma(\theta)$.⁵ Cross sections have also been obtained for the cluster of unresolved states ($E_x=1.769$ to 2.334 MeV—second peak from the right in Fig. 2) which essentially represents the 1^+ member of the $(\pi g_{7/2}, \nu g_{7/2}^{-1})$ multiplet.⁷

The resulting angular distributions are presented in Fig. 3. The 0^+ IAS data have also been included to indicate the sensitivity of the (p,n) reaction to the multipolarity of the transition. The similarity in shape of $\sigma(\theta)$ for the known $(\pi g_{7/2}, \nu g_{7/2}^{-1})_{1^+}$ excitation and the broad peak obviously suggests a 1^+ assignment for the latter.

Of the available particle-hole configurations which can couple to 1^+ , only $(\pi g_{7/2}, \nu g_{7/2}^{-1})$ is expected to have the observed excitation energy.⁸ The curved line in Fig. 3 is a microscopic DWBA prediction (including the knockon exchange amplitude) of the (p,n) cross section for $(\pi g_{7/2}, \nu g_{7/2}^{-1})_{1^+}$ excitation from a closed-shell ^{90}Zr core. This calculation is based on an effective nucleon-nucleon interaction⁵ derived from a G-matrix for the Reid soft-core potential. The term proportional to $\hat{d}_i \cdot \hat{d}_j \hat{T}_i \cdot \hat{T}_j$ is primarily responsible for the theoretical cross section, although the tensor component also makes an appreciable contribution. We consider the experimental cross section and the calculation to agree within the uncertainty in the effective interaction (note

$\sqrt{0.3}(\pi g_{7/2}, \nu g_{9/2}^{-1})_1^+ - \sqrt{0.1}(\pi g_{9/2}, \nu g_{7/2}^{-1})_1^+$, which should account for 90% of the $(\pi g_{7/2}, \nu g_{9/2}^{-1})_1^+$ strength accessible to a direct (p,n) reaction. Furthermore, the anti-analog should be roughly 7 MeV¹³ below the analog of the GMD, in agreement (considering the uncertainty in the isospin splitting) with the observed excitation energy of the broad peak. If additional configurations, e.g. $(\pi g_{9/2}^{-1})_1^+$, are considered in the ⁹⁰Zr ground state, the GMD will have several anti-analogs, the highest-lying one of which will contain a coherent mixture of 1p-1 excitations responsible for the broad peak.

Thus, we observe structure in (p,n) spectra which, at least for ⁹⁰Zr, is consistent with a simple spin- and isospin-flip of the available neutrons. Such transitions correspond to both the giant Gamow-Teller resonance and the anti-analog of the giant magnetic-dipole resonance.

that the factor of 1.5 increase in the theoretical cross section displayed in Fig. 3 corresponds to only a 22% renormalization of the interaction). In the closed-shell model of ⁹⁰Zr, the entire strength of the Gamow-Teller operator $(\tau_i^+ \tau_i^-)$ is exhausted by the $(\pi g_{7/2}, \nu g_{9/2}^{-1})_1^+$ excitation. Thus, the magnitude of the observed peak is consistent with the Gamow-Teller sum rule.

The obvious similarity in the target subspace of t_{11} and the Gamow-Teller operator insures that their strength functions are roughly proportional. This has been recently verified⁹ in the (⁶Li, ⁶He) charge-exchange reaction, which is undoubtedly much less direct than (p,n).

The magnetic-dipole operator is also closely related to t_{11} . The correspondence between their strength functions has been demonstrated in both (t, ³He)¹⁰ and (n,p)¹¹ reactions. Again in the closed-shell model of ⁹⁰Zr, the giant magnetic-dipole resonance (GMD) is equivalent to the $(\nu g_{7/2}^{-1})_1^+$ excitation. The spin-orbit splitting plus the repulsive residual interaction between the $g_{7/2}$ neutron and the $g_{9/2}$ neutron hole is approximately 9 MeV.⁸ A broad structure thought to be the GMD has been observed¹² at this excitation energy in ⁹⁰Zr(e,e') at $\theta=180^\circ$ with 80.6-MeV/c electrons. The isobaric analog of this state should be about 9 MeV above the IAS in ⁹⁰Nb. In the simple model, the analog of the GMD is $\sqrt{0.1}(\pi g_{7/2}, \nu g_{9/2}^{-1})_1^+ + \sqrt{0.3}(\pi g_{9/2}, \nu g_{7/2}^{-1})_1^+$, which is predominantly 2p-2h and, thus, weakly excited by a one-step process. However, the anti-analog of the GMD is

REFERENCES

1. A. deshalit and H. Feshbach, Theoretical Nuclear Physics, vol. 1, pp. 798-805 (New York, Wiley, 1974); M. Morita, et al., Prog. Theor. Phys. Suppl. 48, 41(1971).
2. J.D. Anderson and C. Wong, Phys. Rev. Lett. 7, 250(1961).
3. K. Ikeda, S. Fujii, and J.I. Fujita, Phys. Lett. 3, 271(1963).
4. J.C. Hardy, in Nuclear Spectroscopy and Reactions, Part C, ed. by J. Cerny, p. 417 (New York, Academic Press, 1974).
5. R.R. Doering, D.M. Patterson, and Aaron Galonsky, Phys. Rev. C12, 378(1975).
6. Compare with the relatively large two-step EAS cross sections for (p,n) at $E_p \approx 18$ MeV in V.A. Madsen and M.J. Stomp, Phys. Rev. Lett. 28, 629(1972).
7. J.A. Cooper, J.M. Hollander, and J.O. Rasmussen, Nucl. Phys. A109, 603(1968).
8. F.E. Cecil, T.T.S. Kuo, and S.F. Tsai, Phys. Lett. 45B, 217(1973); S.F. Tsai, private communication.
9. W.R. Wharton and P.T. Debevec, Phys. Rev. C11, 1963(1975).
10. E.R. Flynn, J. Sherman, and N. Stein, Phys. Rev. Lett. 32, 846(1974).
11. M. Obu and T. Terasawa, Prog. Theor. Phys. 43, 1231(1970).
12. L.W. Fagg, Rev. Mod. Phys. 47, 683(1975); L.W. Fagg, private communication.
13. G.F. Bertsch and A. Mekjian, Ann. Rev. Nucl. Sci. 22, 25(1972).

FIGURE CAPTIONS

Figure 1.--Neutron time-of-flight spectrum at $\theta=0^\circ$ for $^{90}\text{Zr}(p,n)^{90}\text{Nb}$ at $E_p=35$ MeV. Expected EAS positions are labeled with the excitation energies of the parent analog states in ^{90}Zr .

Figure 2.--Differential cross section vs. neutron energy for $^{90}\text{Zr}(p,n)^{90}\text{Nb}$ at $E_p=45$ MeV and $\theta=0^\circ$. The straight line represents a background fit to regions adjacent to the broad peak and IAS. *The enhancement is centered 2 at 8.4 MeV in ^{90}Nb*
 Figure 3.-- $\sigma(\theta)$ for the broad peak at the expected $(\pi g_7/2, \nu g_7/2)_{1^+}$ excitation energy in the $^{90}\text{Zr}(p,n)^{90}\text{Nb}$ spectra taken at $E_p=45$ MeV compared with known 0^+ and 1^+ experimental angular distributions and with a microscopic DWBA calculation (curved line).

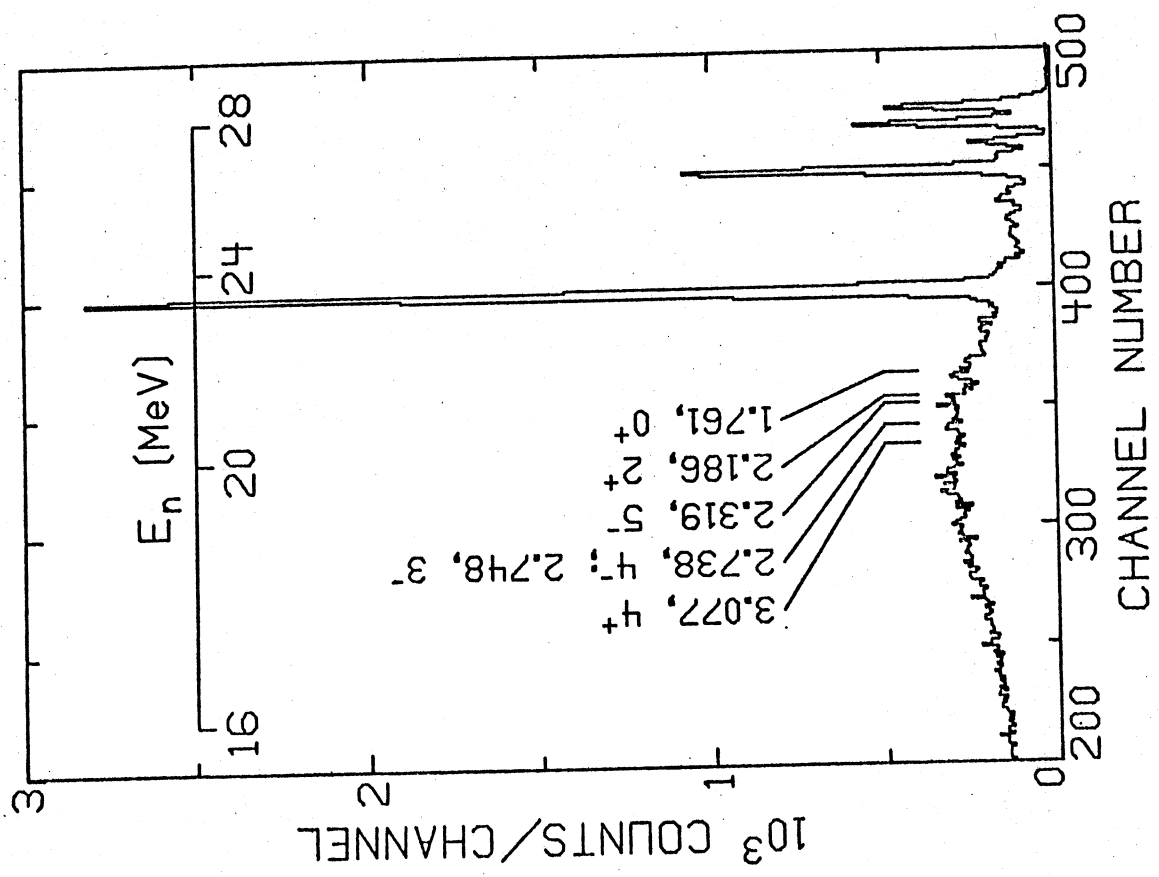


Fig. 1

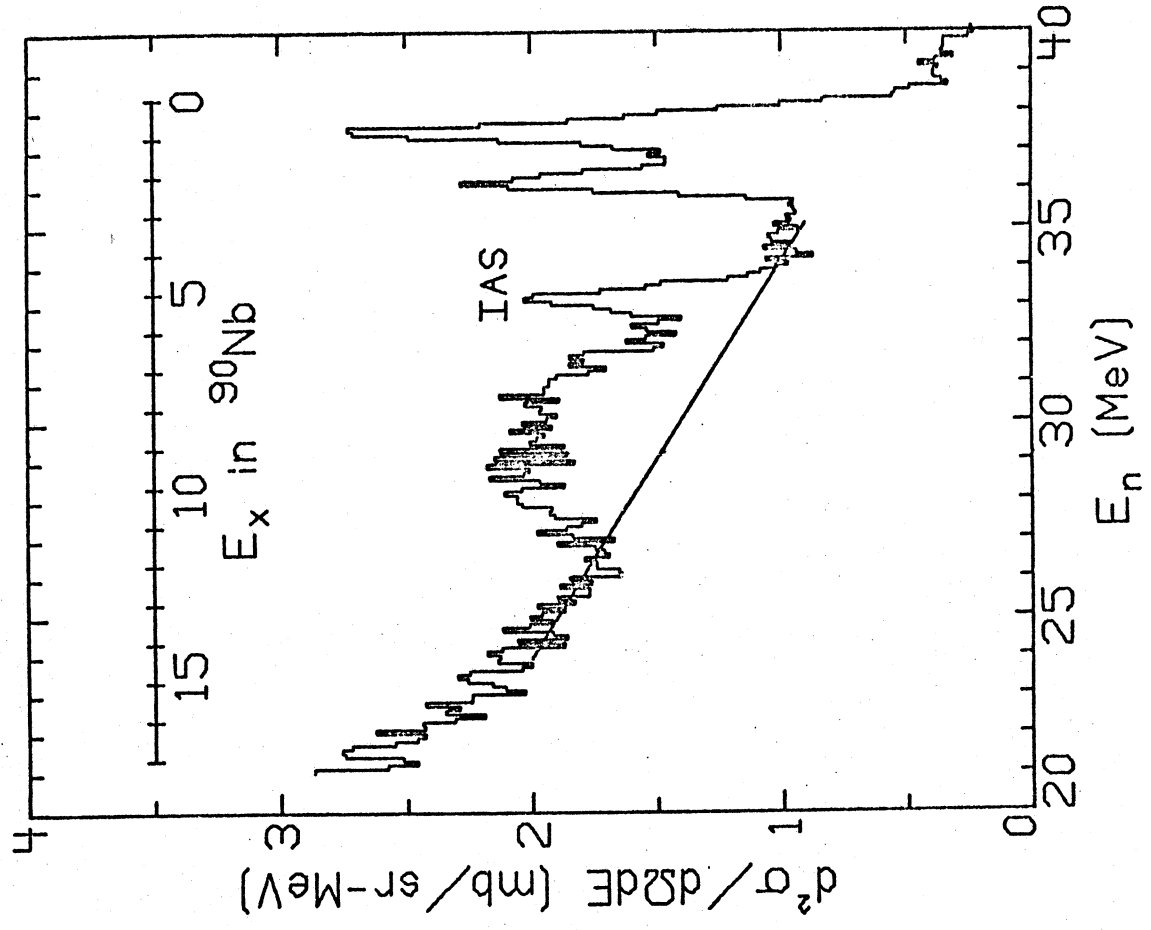


Fig. 2

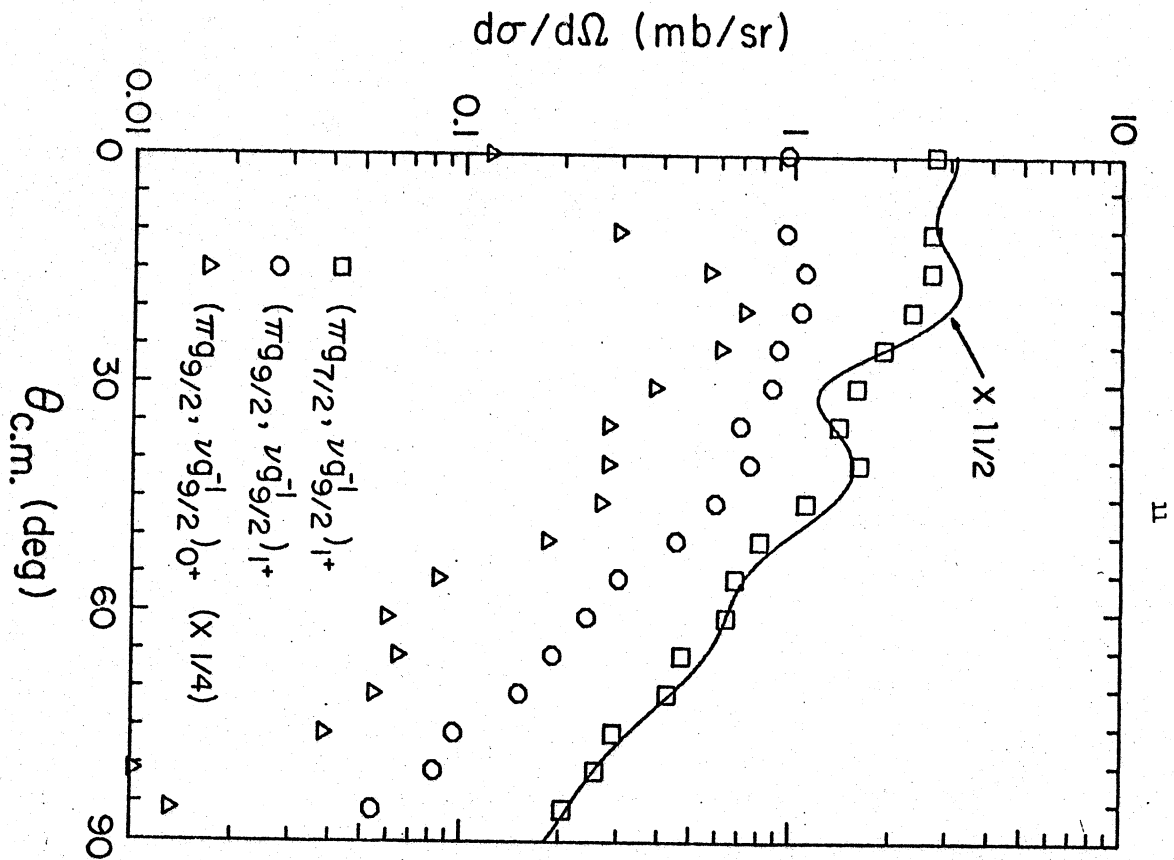


Fig. 3